AIP Journal of Applied Physics

Plasma-enabled growth of ultralong straight, helical, and branched silica photonic nanowires

S. Y. Huang, K. Ostrikov, and S. Xu

Citation: Journal of Applied Physics **104**, 033301 (2008); doi: 10.1063/1.2963694

View online: http://dx.doi.org/10.1063/1.2963694

View Table of Contents: http://scitation.aip.org/content/aip/journal/jap/104/3?ver=pdfcov

Published by the AIP Publishing

Plasma-enabled growth of ultralong straight, helical, and branched silica photonic nanowires

S. Y. Huang,[1] K. Ostrikov,[2,3,a)] and S. Xu[1]
[1]*Plasma Sources and Applications Center, Nanyang Technological University, Singapore 637616, Singapore*
[2]*Plasma Nanoscience, School of Physics, The University of Sydney, Sydney, New South Wales 2006, Australia*
[3]*CSIRO Materials Science and Engineering, Lindfield, New South Wales 2070, Australia*

(Received 30 April 2008; accepted 30 May 2008; published online 1 August 2008)

This article reports on the low-temperature inductively coupled plasma-enabled synthesis of ultralong (up to several millimeters in length) SiO_2 nanowires, which were otherwise impossible to synthesize without the presence of a plasma. Depending on the process conditions, the nanowires feature straight, helical, or branched morphologies. The nanowires are amorphous, with a near-stoichiometric elemental composition ([O]/[Si]=2.09) and are very uniform throughout their length. The role of the ionized gas environment is discussed and the growth mechanism is proposed. These nanowires are particularly promising for nanophotonic applications where long-distance and channelled light transmission and polarization control are required. © *2008 American Institute of Physics*. [DOI: 10.1063/1.2963694]

I. INTRODUCTION

Ultralong one-dimensional (1D) nanostructures such as nanowires (NWs) and nanotubes have recently been the subject of a significant research interest due to their ability for effective electron confinement in two dimensions as well as highly unusual structural, electrical, mechanical, thermoelectric and piezoelectric, optoelectronic, and other properties.[1–10] Such properties are extremely promising for a large number of advanced technological applications ranging from structural reinforcements to ultrasensitive gas sensors and integrated nanoelectronics.[2,4,8,9] These 1D objects can reach macroscopic sizes in one dimension and as such are particularly appealing for light-guiding and multiplexing photonic on-chip functionalities and devices.[11,12]

To enable the above applications, the 1D nanostructures should meet certain requirements. For example, for nanoelectronic applications, such objects should be conducting and be able to carry a large current without major Ohmic losses.[13] On the other hand, for photonic applications they should be optically transparent and introduce negligibly low optical losses along the way of guided light.[11,12] More complex functionalities such as multiplexers and directional couplers require branched ultralong wires. In many cases, the ultralong wires need to be directed and stretched along a flat substrate of the chip. Previous reports on relevant 1D nanostructures include but are not limited to ultralong single walled carbon nanotubes and various metal oxide and semiconducting (e.g., ZnO, silicon-based, etc.) NWs (see Refs. 1–19 and references therein).

Despite a very large number of relevant reports, controlled and predictable synthesis of 1D objects capable of meeting the above requirements still remains one of the major challenges for nanoscale design and fabrication. This is particularly challenging for highly promising and cost-effective approaches based on bottom-up NW assembly.[2,3,18,19] One of the greatest difficulties in this regard is to be able to align the wires along the substrate and provide appropriate conditions for their uninterrupted growth. These conditions can be met using "bottom-up" catalyzed synthesis of NWs, provided that metal catalyst nanoparticles (NPs) can be shed and lifted off the substrate surface and remain at the NW tip. In this case, source materials precipitate through the catalyst NPs to form a 1D structure underneath; if this growth is not interrupted, it becomes possible to grow very long 1D wires.

However, the NW growth appears to be extremely vulnerable to poisoning and/or blockage of the catalyst NP by the precipitating material (see review article[2] and references therein). Therefore, to prevent the undesirable growth interruption, the catalyst NPs should ideally be treated in a "self-cleaning" environment. The ideal environment should not be very reactive (to avoid significant chemical modification of the catalyst and the NWs) yet be able to provide continuous conditioning of the NP at NW surfaces.

As suggested by the results of this work, thermally nonequilibrium low-temperature plasmas are good candidates for this purpose. More specifically, it will be shown that plasma conditions of low-temperature plasma discharges sustained with reasonably low rf power in a mixture of silane, oxygen, and argon gases are very favorable to synthesize not only ultralong high-quality amorphous silica NWs, but also create branched and helical wires. More importantly, it was not possible to grow these structures under the same process conditions without the aid of the inductively coupled rf plasma.

In this article, we propose mechanisms that explain how an ionized gas environment enables the growth of ultralong NWs and, in particular, during the metal catalyst lift-off phase and in the process of continuous clean up of the NW tip during the subsequent growth process. We also address the issue why some of the wires tend to form branched struc-

[a)]Electronic mail: k.ostrikov@physics.usyd.edu.au.

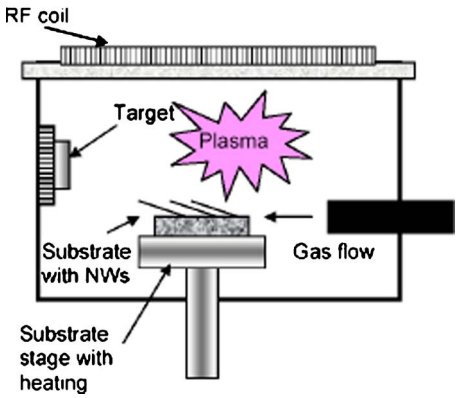

FIG. 1. (Color online) Schematics of the experimental facility used for SiO_2 NW synthesis.

tures. Examples of more sophisticated helical silica nanocoils and twisted wires are given as well. These 1D nanostructures can in principle be used to control light polarization as it propagates along the wires. This article is structured as follows. In Sec. II, most important experimental details are provided. The experimental results on the growth of SiO_2 NWs under different process conditions are presented and summarized in Sec. III. In Sec. IV, the results obtained are discussed and the growth models of the NWs of various morphologies are proposed. Specific attention is paid to the explanation of how the plasma environment enabled the growth of very long silica NWs, which were impossible to synthesize under similar process conditions using neutral gas-based chemical vapor deposition (CVD). Section V summarizes the main findings of this work and gives an outlook for future work in this direction.

II. EXPERIMENTAL DETAILS

The experiments were conducted in the Integrated Plasma-Aided Nanofabrication Facility (IPANF) and are described in detail elsewhere.[20–22] Figure 1 shows a schematic diagram of the experimental setup for the growth of 1D nanostructures. The base pressure in the reactor chamber was maintained in the 10^{-5} Pa range. Silane (SiH_4) and oxygen were used as source gases to synthesize the SiO_2 NWs. Both reactive gases were moderately diluted in inert argon gas. The pressure of the gas mixture varied from 20 to 50 mTorr. Polished Si(100) wafers were used as the growth substrates. The substrates were preheated to the fixed temperature (T_s =650 °C, where T_s is the surface temperature) before the gas mixture was let in the chamber. Prior to the NW growth, a 10-nm-thick nickel catalyst film was deposited onto the growth surface using inductively coupled plasma (ICP)-assisted rf magnetron sputtering of a high-purity Ni target. The frequency of the rf generator connected to the magnetron-target assembly was 13.56 MHz. In the catalyst preparation processes, the rf power (typically 100–150 W) was applied to the sputtering target shortly before the gas inlet. The growth process of SiO_2 NWs, in both neutral gas-based and plasma-assisted cases, typically lasted from 5 to 30 min. The SiH_4+O_2+Ar gas mixture was delivered through a nozzle which created a gas flow parallel to the substrates as shown in Fig. 1.

A specific arrangement was made to investigate the effect of the plasma environment on the growth process of the SiO_2 1D nanostructures. After the gas mixture was let into the chamber, a low-frequency ICP discharge was ignited by applying approximately 600–800 W of rf power generated by a 460 kHz rf generator. The rf power is delivered to the reactor chamber from a flat spiral inductive antenna located slightly above a vacuum-tight fused silica window on top of the chamber. Previous reports suggest that this experimental arrangement is particularly useful to enhance the growth and improve the properties of various nanostructures of different dimensionality and nanostructured films.[19,23–28] During the plasma-assisted deposition process, the substrate holder was electrically insulated from the main chamber; no external bias was used in this series of experiments. However, there exists a small floating potential between the plasma bulk and the surface due to the plasma sheath effect. High-resolution scanning electron microscopy (SEM) imaging was conducted with the aid of a JEOL JSM 6500F field-emission scanning electron microscope. Transmission electron microscopy (TEM), including high-resolution TEM (HRTEM), has been performed using a Philips FEG CM300 electron microscope equipped with a 200 kV field emission gun. The elemental composition of the NWs was examined using an energy dispersive x-ray (EDX) spectrometer (OXFORD INCA x-sight 7421) attached to the TEM.

III. EXPERIMENTAL RESULTS

The main experimental observations of this work can be summarized as follows.

(i) Without the plasma (only the SiH_4+O_2+Ar neutral gas mixture introduced), no distinctive features were observed on the substrate surface, which was covered with shapeless bulk deposits.
(ii) Introduction of the Ni catalyst led to the growth of nanorodlike structures; however, the length of such nanostructures never exceeded a few hundred nanometers. It was also observed that these nanorods were usually coated by bulk material and no catalyst particles were seen
(iii) The ignition of the plasma discharge changed the situation dramatically: it became possible to synthesize ultralong straight and twisted NWs with some examples shown in Fig. 2.

Moreover, under the plasma-on conditions, the typical sizes of the SiO_2 NWs ranged from a few microns to a couple of millimeters, with some of the wires stretching across the samples. Some of the wires were able to grow perpendicularly and above ("pass over") the intentional scratches on the substrate. Whenever it was possible to observe the NW tips (since most of the wires spanned well outside the SEM scanned area), darker and more contrasted areas near the tips indicated the presence of the Ni catalyst NPs in those areas. Most of the wires grew parallel or almost parallel to the substrate surface without actually touching it. The growth direction of the straight wires was almost the

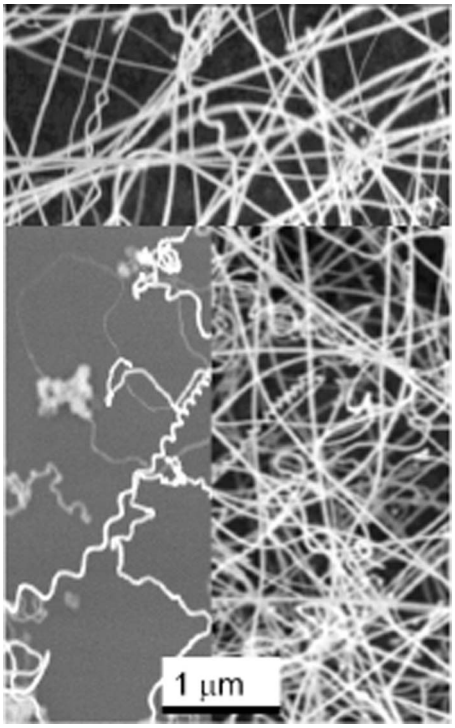

FIG. 2. SEM imaging of long silica NWs grown on a silicon substrate in the ICP-assisted catalyzed CVD in the SiH_4+O_2+Ar gas mixture.

same as the direction of the gas flow from the inlet nozzle. This tendency was even more pronounced as the nozzle was moved closer to the substrates.

The nozzle position also played a significant role in determining the morphology of the 1D nanostructures. When the distance between the nozzle opening and the substrate edge was 10 cm, the NWs showed the tendency to align along the flow direction more clearly. However, when the nozzle was moved a further 5 cm away from the substrates, the growth directions became more random. Moreover, this change in the experimental conditions resulted in the appearance of new helical and twisted morphologies with the representative examples shown in Fig. 3. Figure 3(a) shows a compactly twisted silica nanocoil with the wire thickness of approximately 30 nm and the coil pitch not exceeding 100 nm. Another example of a regular morphology is displayed

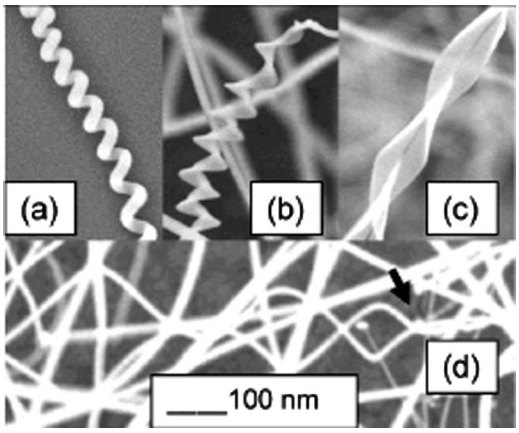

FIG. 3. Representative SEM micrographs of helical [(a)–(c)] and branched (d) silica NWs.

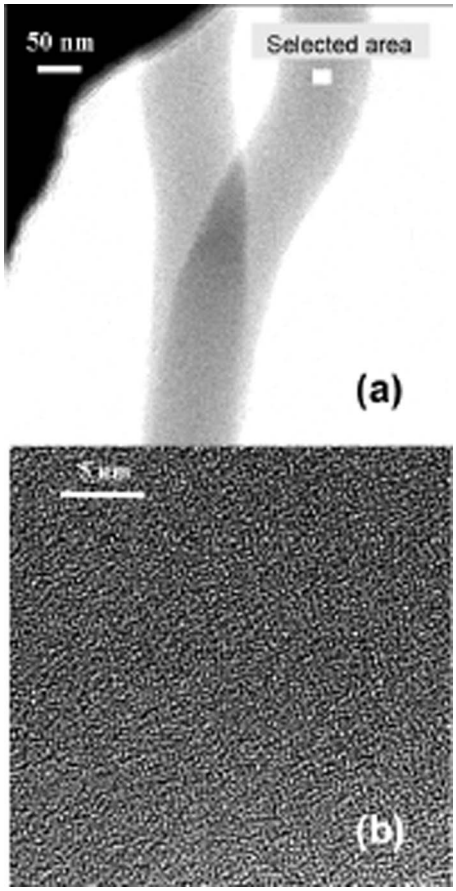

FIG. 4. TEM (a) and HRTEM (b) images of a branched *Y*-junction SiO_2 NW.

in Fig. 3(b) where one can see another nanocoil with edged turns, which are twisted and pointed like in a drill. In this case, the cross section of the coil turns is rectangular with a thickness near the edges of approximately 10 nm. The number of "threads" in the nanocoil, shown in Fig. 3(b), is approximately 9–11 per 1 μm. In some cases, the threadlike 1D nanostructures featured larger pitches and even thinner "blades," as shown in Fig. 3(c). More importantly, the structures displayed in Fig. 3(c) look as if they were made of two interwoven left- and right-hand twisted threads. This appears to be in a stark contrast with the nanocoils shown in Figs. 3(a) and 3(b), which represent a single wire twisted in one direction.

Figure 3(d) shows an example of a *Y*-junction NW with a straight trunk and two branches twisted in the opposite directions. The wire thickness typically ranged from 20 nm [this case is shown in Fig. 3(d)] to 120 nm [Fig. 4(a)]. An interesting feature of the *Y*-junction wire in Fig. 3(d) is the double spiral-like unwinding helix with an increasing pitch. As one can see from Fig. 3(d), the two branches are twisted in the opposite directions.

The *Y*-junction branched NWs were subject to further morphological, structural, and compositional analysis. The results of this analysis are shown in Figs. 4 and 5. Figures 4(a) and 4(b) show the low- and high-resolution TEM micrographs of one of the thickest *Y*-junction NWs. The most striking observation in Fig. 4(a) is that the thickness of the

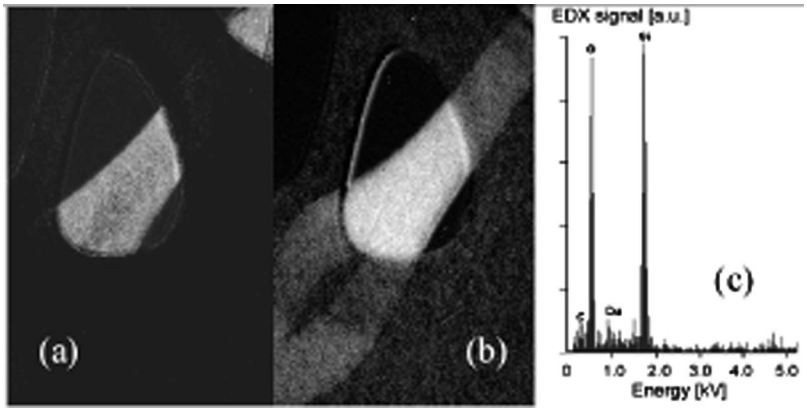

FIG. 5. Chemical mapping of silicon (a) and oxygen (b) in a branched *Y*-junction NW and a representative EDX spectrum collected from the NW structures placed on a copper grid for TEM analysis.

NW trunk is almost the same as the thickness of the branches, with the actual difference not exceeding 5%–10% in most cases. A darker area in Fig. 4(a) is most likely due to the overlap of the two branches as they evolve from the same NW trunk. This is an indication that the NW branching in this case is a relatively smooth process, in contrast to the case of *Y*-junction nanotubes where the splitting of one tubing into two "sleeves" may happen fairly abruptly, especially under the action of external radiation.[29–31] A HRTEM image in Fig. 4(b) shows that the NWs have a very clear and uniform amorphous structure. This image was taken from the selected area on one of the branches marked by a white square in Fig. 4(a).

Another important experimental result is that the SiO_2 NWs appear to be perfectly stoichiometric. The atomic oxygen to silicon ratio ([O]/[Si]) is 55.2%/26.4%=2.09, which is very close to the stoichiometric value of SiO_2 of [O]/[Si]=2:1. Moreover, the elemental composition remains stoichiometric throughout the entire length of the wire, both in the trunk and the branches. The results of chemical mapping suggest that silicon [Fig. 5(a)] and oxygen [Fig. 5(b)] are homogeneously distributed throughout the entire structure of the NW. The EDX analysis also confirms the good chemical purity of the NWs. Indeed, from Fig. 5(c) one can see that the nanostructures are composed of silicon and oxygen only. Minor traces of copper and carbon originate from the TEM grid used in the analysis.

IV. DISCUSSION

Let us now discuss the experimental observations and in particular, the role of the plasma environment and gas flow in the growth of ultralong silica NWs of different morphologies. The fact that no nanostructures were grown without the addition of a catalyst clearly suggests that NW growth is an essentially a catalyzed process. Indeed, catalyst NPs are required to give the appropriate shape to the emerging nanostructures and guide their 1D growth in a specified direction.[2,32] Catalyst particles also reduce energy barriers for the incorporation of building units, which can pass either through the bulk or the surface of the NP before incorporating into the NW structure. The location of the catalyst particle plays an important role in the growth process.[33] If the metal catalyst NP is anchored to the substrate, the new building units (Si and oxygen atoms in the case considered) have to reach the NW base no matter how long it is.[6] On the other hand, if a metal NP is located at the NW tip, any suitable building units need to reach the NW tip to be able to be extruded through the NP and nucleate underneath effectively, thus moving the catalyst further away from the base and eventually elongating the NW.

In our experiments, addition of the nickel catalyst effected a significant change at the early growth stage giving rise to nanorodlike structures. However, these nanorods were covered by and in some cases even buried in presumably amorphous material. The observation that no catalyst particles were seen at the NW tips suggests that it is very likely that the nickel NPs remained attached to the substrate. This also indicates that the growth process may have terminated when the catalyst particles were completely covered by the deposited material. In this case, the incoming Si and O building units were apparently unable to incorporate into the developing structure, which immediately resulted in termination of the NW growth. Numerous amorphous deposits between the wires and on their lateral surfaces suggest the possibility of random attachment of the deposited material without the formation of any regular layers at the outer surfaces of the NWs. Nevertheless, these results suggest that it is indeed possible to synthesize silica nanorods in a catalyzed CVD process. However, our earlier experiments suggest that the surface temperature should be reasonably high to initiate the growth process.[20,25] Such high temperatures are required for dissociation of the silane carrier gas on a hot solid surface and also to increase the mobility of adatoms to enable them to overcome the incorporation barriers and contribute to the NW growth. This fact dictated our choice of the surface temperature in this series of experiments.

As can be seen from Figs. 2–5, after the external ICP discharge was ignited, the NW growth process changed dramatically. The most important effect of the plasma environment was the possibility to grow ultralong silica NWs. The most likely common causes for this dramatic change in the NW growth behavior are related to the combination of the following factors:

(i) repositioning of the catalyst particles to the tip sections of the NWs,
(ii) increased rates of building unit creation and delivery to the nucleation and growth sites underneath the

catalyst NPs, which eventually results in the higher growth rates, and

(iii) reduced contamination and poisoning of the catalyst, which leads to an improved ability of the NPs to accept and transport the silicon and oxygen building units on their surfaces and within their bulk.

Let us now examine how the ignition of the plasma discharge may have created favorable conditions to meet the above causes (i)–(iii). First of all, the observation of nickel NPs on the NW tips evidences the possibility of the NP lift-off from the surface during the NW nucleation stage. A quite similar effect has been frequently reported in the plasma-assisted catalyzed synthesis of carbon nanofibers and multiwalled nanotubes, which in most cases proceeds via the tip growth scenario.[34,35] The electric charge accumulated on both the catalyst particles and the substrate plays a prominent role in the NP lift-off process. Indeed, at the beginning of the growth process, the catalyst NP is affected by a strong push of the extruded and nucleated species of the building material, which tend to attach to the substrate underneath the NP. This creates a significant pressure, which leads to the NP elongation. Extrusion of the building material through the substrate-facing surfaces of the NP leads to the initial nucleation of the NW trunk between the catalyst and the substrate. This leads to the reshaping of the NPs, which often become pearlike shaped with the narrower part still attached to the substrate.

In a low-temperature plasma, both the NP and the substrate acquire a negative electric charge.[6] This effect is particularly clear in the case considered when the substrate surface was maintained at the floating potential. As the NP elongates and reshapes, additional electrostatic repulsion between the substrate and the NP may lead to detachment of the catalyst particles from the surface; in this case, the NWs grow in the tip-growth mode. Therefore, it is indeed possible that after the plasma discharge was started, conditions became favorable for the catalyst NPs to be located at the NW tips [condition (i)] rather than at their bases, which was the case in the neutral CVD.

Regarding condition (ii), a plasma discharge significantly increases the rates of dissociation of silane and oxygen molecules in the gas phase as compared to thermal dissociation on hot solid surfaces, which appears to be the only option in most thermal CVD processes.[36,37] In the case considered (surface temperature of 650 °C), the fraction of silicon atoms with no or a small number of hydrogen atoms (which are most suitable for the synthesis of SiO_2) is expected to be quite low. On the other hand, silyl (SiH_3) and siluene (SiH_2) radicals (which are more plentiful under thermal CVD conditions) have a strong tendency to polymerize and form bulk films or nano-/microparticles.[38] When the plasma discharge is turned on, the rates of dissociation of silane and oxygen molecules increase. A most dramatic increase (by several orders of magnitude) happens in the gas phase, mostly due to the electron impact dissociation and dissociative collisions of radicals, which is only possible in an ionized medium.

Another effect exerted by the plasma is additional surface heating, which leads to even higher rates of production of silicon and oxygen on the hot surface. Under conditions of heavy ion bombardment, the additional plasma-related increase of the surface temperature can be as high as 100–150 °C.[6,34,39] In the case considered, however, this effect is unlikely to be very strong since the surface was maintained under the floating potential, which usually does not exceed ~10 V. Furthermore, high-rate recombination of reactive radicals (e.g., recombination of two oxygen atoms to form O_2 molecule) on the solid surface may lead to additional substantial increases of the surface temperature as compared to the neutral CVD case.[40] It is important to stress, however, that the rf input power P_{in} that was used to sustain the discharge was relatively low (600–800 W) as compared to the synthesis of polycrystalline silicon films for solar cell applications under very similar gas pressures using the same feedstock gases. Thus, it is quite possible that gas-phase silane polymerization was not effective in the case considered. A common consequence of this polymerization is the formation of silane nanopowder particles,[41,42] which clearly was not the case in our experiments (almost all NWs were clear of NP contamination).

Another indication of the importance of the plasma-induced gas-phase dissociation is that the catalyst NPs are attached to the growth ends of the NWs which are apparently lifted off the surface and float in the gas flow which bends the NWs toward the substrate surface. Therefore, as the NWs grow longer, it becomes more difficult for the building units created on the hot solid surface to travel all the way to the catalyst particle along the entire NW length to participate in the growth process. Therefore, the species which either deposit directly onto the NW tip from the gas phase or arrive from not-so-remote areas on the lateral surface are expected to make the major contribution to the growth process. The probability of this focused deposition near the tips of 1D nanostructures significantly increases in the plasma environment.[43,44]

Moreover, the electric field lines converge near the NW sharp tips and draw ion fluxes onto the catalyst NPs located exactly in those areas. This ion bombardment, nonexistent in the neutral CVD case, leads to two additional effects that further facilitate the growth of ultralong NWs. First, this leads to continuous conditioning of the catalyst surface and removal of any unwanted deposits, which may block the open surface of the catalyst NPs and eventually completely disrupt the growth process. This certainly improves the chances of the incoming building units to access the catalyst NPs and eventually the nucleation sites underneath. Another real possibility is that focused ion fluxes substantially increase the rates of dissociation of silane and oxygen molecules on the catalyst surface. A similar possibility has been reported previously for the case of plasma-assisted synthesis of carbon nanofibers in the tip growth mode.[35,45] What is even more important is that additional ion bombardment may substantially increase the temperature of the catalyst NP. Due to a very small size of the nickel NP, chances of it to have reasonably high temperatures are higher as compared with the bulk substrate. This higher temperature leads to better solubility of silicon and oxygen in nickel as well as higher

rates of diffusion of building units through the catalyst. A combination of these two factors eventually leads to higher rates of nucleation of silicon and oxygen species at the inner surfaces of the catalyst particle facing the NW. This basically justifies the realization of condition (iii) in the plasma environment.

In the above, we have mentioned that the surface was maintained under the (small) floating potential. This potential and the associated electric field in the plasma sheath were clearly insufficient to enable vertical alignment of the NWs. In fact, a balance of the forces exerted on the NWs by the gas flow (predominantly in the horizontal direction) and by the electric field (predominantly in the vertical direction) forced the NWs to align almost parallel to the surface yet without touching the surface by their tips. Indeed, the repulsive electric force acts as support of the long NWs bent by the gas flow. It is very likely that without the presence of the plasma, the very long NWs would eventually have to touch the surface by their tips. This would almost certainly mean the end of their growth cycle. This plasma- and electric-field-assisted mechanism is quite similar to the "kite mechanism" successfully used to explain the growth of ultralong carbon nanotubes in the "fast-heating" CVD process[16] wherein convection fluxes were used to support the NWs floating slightly above the substrate surface. Without this fast heating process and the associated convection flows, CVD-grown NWs often bend toward the surface under the action of van der Waals forces. The growth process stops as soon as the NW tip gets in contact with the surface. In our case, the substrate heating was continuous, which does not create suitable conditions for the existence of any significant uprising convection flows that can support the NWs as they elongate.

To end Sec. IV, we state that a detailed explanation of the growth kinetics of helical and branched NWs shown in Fig. 3 was not the purpose of this article. Here we only stress that any specific morphology shown in Figs. 3(a)–3(d) can be regarded as the result of action of two main factors: the direction and magnitude of the resultant force at every particular point along the NW and a specific rearrangement (e.g., splitting or reshaping) of the catalyst NP. Indeed, a combination of the gas drag, convection, electric, and van der Waals forces may determine the distribution of internal stresses, which in turn may affect the most energetically favorable arrangement (e.g., reshaping) of the catalyst NP. For example, if the NP is cubic and the rates of diffusion of the building material through one of the three facets are much higher than through the other two facets, one could expect the growth of straight wires shown in Fig. 2. If the NP is elongated along one direction and is very thin along the other one, one could expect the growth of drill-like wires with relatively thin thread blades shown in Fig. 3(b). A quite similar mechanism was invoked to explain different morphologies of carbon microcoils.[46]

The mechanism of formation of branched helical NWs still remains unclear at this stage. It is very likely that the branching happens because of splitting of the catalyst NP into two; each of the two fragments controls the growth of each branch. In some cases, one of the branches was observed significantly shorter than the other. This observation indicates either uneven splitting of the catalyst particle (so that catalytic activity of a Ni NP in one of the branches was much weaker) or cluttering/poisoning of the catalyst particle in the shorter branch. Both experimental and simulation work is underway to clarify this issue.

V. CONCLUSION

The results of this work suggest that the low-temperature thermally nonequilibrium plasma environment has enabled the growth of ultralong silica NWs, which was clearly impossible in the uncatalyzed and neutral gas-based catalyzed process. This became possible because of a combination of various plasma-related effects, such as enhanced production of suitable building units, creating appropriate conditions for high-rate incorporation of these building units through the catalyst NPs into the growing NWs, continuous conditioning of the open catalyst surface while the NWs grow, lifting off the catalyst NP from the substrate surface due to electrostatic interactions, balancing of the "supporting" electrostatic force and the force of the gas drag, focusing of ion beams toward the tips of the growing NWs, increased temperature and hence reactivity of the catalyst, and some others. This eventually made it possible to grow ultralong silica NWs of different sizes and morphologies. The elemental composition of the NWs is very close to the stoichiometry; moreover, silicon and oxygen elements are distributed very homogeneously throughout the wires. The SiO_2 NWs are amorphous and have diameters typically ranging from 20 to 120 nm. Different morphologies, such as nanocoil-like, single and double-helical, drill-like, and helical branched NWs have been observed as well. These NWs can be used in a range of advanced applications and are particularly promising for applications as light-guiding and multiplexing structures. Future work will be focused on the development of growth models and supporting numerical simulations to explain the link between the plasma-related process parameters and the observed complex morphologies.

ACKNOWLEDGMENTS

This work was partially supported by the A*STAR and NRF (Singapore), the Australian Research Council, and CSIRO. Assistance of J. D. Long in setting up the experimental facility and helpful discussions are gratefully acknowledged.

[1] W. Kratschmer, L. D. Lamb, K. Foristopnlos, and D. R. Huffman, Nature (London) **347**, 354 (1990).
[2] W. Lu and C. M. Lieber, J. Phys. D **39**, R387 (2006).
[3] U. Cvelbar and M. Mozetic, J. Phys. D **40**, 2300 (2007).
[4] A. Borrás, A. Barranco, F. Yubero, and A. R. González-Elipe, Nanotechnology **17**, 3518 (2006).
[5] M. Keidar, J. Phys. D **40**, 2388 (2007).
[6] K. Ostrikov, Rev. Mod. Phys. **77**, 489 (2005).
[7] H. W. Wei, C. H. Tung, M. S. Sung, K. C. Leou, and C. H. Tsai, J. Appl. Phys. **102**, 114306 (2007).
[8] U. Cvelbar, K. Ostrikov, A. Drenik, and M. Mozetic, Appl. Phys. Lett. **92**, 133505 (2008).
[9] A. B. Greytak, L. J. Lauhon, M. S. Gudiksen, and C. M. Lieber, Appl. Phys. Lett. **84**, 4176 (2004).
[10] E. N. Dattoli, Q. Wan, W. Guo, Y. B. Chen, X. Q. Pan, and W. Lu, Nano Lett. **7**, 2463 (2007); S. Kodambaka, J. Tersoff, M. C. Reuter, and F. M. Ross, Science **316**, 729 (2007), and the references therein.

[11]M. A. Foster, A. C. Turner, M. Lipson, and A. L. Gaeta, Opt. Express **16**, 1300 (2008).
[12]S. J. Pearton, D. P. Norton, and F. Ren, Small **3**, 1144 (2007).
[13]W. Lu and C. M. Lieber, Nat. Mater. **6**, 841 (2007).
[14]M. Keidar, I. Levchenko, T. Arbel, M. Alexander, A. M. Waas, and K. Ostrikov, Appl. Phys. Lett. **92**, 043129 (2008).
[15]X. Q. Pan, J. Jiang, Y. J. Zeng, H. P. He, L. P. Zhu, Z. Z. Ye, B. H. Zhao, and X. H. Pan, J. Appl. Phys. **103**, 023708 (2008).
[16]S. Huang, M. Woodson, R. Smalley, and J. Liu, Nano Lett. **4**, 1025 (2004).
[17]L. X. Zheng, M. J. O'Connell, S. K. Doorn, Y. H. Zhao, E. A. Akhadov, M. A. Hoffbauer, B. J. Roop, Q. X. Jia, R. C. Dye, D. E. Peterson, S. M. Huang, J. Liu, and Y. T. Zhu, Nat. Mater. **3**, 673 (2004).
[18]M. Mozetic, U. Cvelbar, M. K. Sunkara, and S. Vaddiraju, Adv. Mater. (Weinheim, Ger.) **17**, 2138 (2005).
[19]K. Ostrikov and A. B. Murphy, J. Phys. D **40**, 2223 (2007).
[20]S. Xu, K. Ostrikov, J. D. Long, and S. Y. Huang, Vacuum **80**, 621 (2006).
[21]K. N. Ostrikov, S. Xu, and A. B. M. S. Azam, J. Vac. Sci. Technol. A **20**, 251 (2002); K. N. Ostrikov, M. Y. Yu, and N. A. Azarenkov, J. Appl. Phys. **84**, 4176 (1998).
[22]I. B. Denysenko, S. Xu, J. D. Long, P. P. Rutkevych, N. A. Azarenkov, and K. Ostrikov, J. Appl. Phys. **95**, 2713 (2004); N. A. Azarenkov, I. B. Denysenko, and K. N. Ostrikov, J. Phys. D **28**, 2465 (1995).
[23]Z. L. Tsakadze, K. Ostrikov, J. D. Long, and S. Xu, Diamond Relat. Mater. **13**, 1923 (2004).
[24]Z. L. Tsakadze, K. Ostrikov, and S. Xu, Surf. Coat. Technol. **191**, 49 (2005); S. Y. Xu, J. D. Long, L. N. Sim, C. H. Diong, and K. Ostrikov, Plasma Processes Polym. **2**, 373 (2005).
[25]K. Ostrikov, J. D. Long, P. P. Rutkevych, and S. Xu, Vacuum **80**, 1126 (2006).
[26]W. Zhou, X. X. Zhong, X. C. Wu, L. Q. Yuan, Q. W. Shu, W. Li, and Y. X. Xia, J. Phys. D **40**, 219 (2007).
[27]E. Tam, I. Levchenko, and K. Ostrikov, J. Appl. Phys. **100**, 036104 (2006).
[28]V. Ligatchev, T. K. S. Wong, B. Liu, and Rusli, J. Appl. Phys. **92**, 4605 (2002); I. Levchenko and K. Ostrikov, J. Phys. D **40**, 2308 (2007).
[29]B. Gan, V. Ligatchev, Q. Zhang, Q. F. Huang, C. Kerlit, S. F. Yoon, Rusli, X. B. Zhang, and W. Z. Li, Mater. Lett. **45**, 315 (2000).
[30]D. Grimm, P. Venezuela, F. Banhart, N. Grobert, H. Terrones, P. A. Ajayan, M. Terrones, and A. Latge, Small **3**, 1900 (2007).
[31]A. V. Krasheninnikov and F. Banhart, Nat. Mater. **6**, 723 (2007).
[32]M. Paladugu, J. Zou, Y. N. Guo, G. J. Auchterlonie, H. J. Joyce, Q. Gao, H. H. Tan, C. Jagadish, and Y. Kim, Small **3**, 1873 (2007).
[33]A. Fontcuberta i Morral, J. Arbiol, J. D. Prades, A. Cirera, and J. R. Morante, Adv. Mater. (Weinheim, Ger.) **19**, 1347 (2007).
[34]M. Meyyappan, L. Delzeit, A. Cassell, and D. Hash, Plasma Sources Sci. Technol. **12**, 205 (2003).
[35]I. Denysenko and K. Ostrikov, Appl. Phys. Lett. **90**, 251501 (2007).
[36]J. H. Song, W. Jo, and N. M. Hwang, Thin Solid Films **515**, 7446 (2007).
[37]N. M. Hwang and D. Y. Kim, Int. Mater. Rev. **49**, 171 (2004).
[38]S. V. Vladimirov and K. Ostrikov, Phys. Rep. **393**, 175 (2004); K. N. Ostrikov and M. Y. Yu, IEEE Trans. Plasma Sci. **26**, 100 (1998).
[39]M. Keidar, Y. Raitses, A. Knapp, and A. M. Waas, Carbon **44**, 1022 (2006).
[40]U. Cvelbar, B. Markoli, I. Poberaj, A. Zalar, L. Kosec, and S. Spaic, Appl. Surf. Sci. **253**, 1861 (2006).
[41]K. Koga, S. Iwashita, and M. Shiratani, J. Phys. D **40**, 2267 (2007).
[42]P. Roca i Cabarrocas, T. Nguyen-Tran, Y. Djeridane, A. Abramov, E. Johnson, and G. Patriarche, J. Phys. D **40**, 2258 (2007).
[43]I. Levchenko, M. Korobov, M. Romanov, and M. Keidar, J. Phys. D **37**, 1690 (2004).
[44]I. Levchenko, K. Ostrikov, and E. Tam, Appl. Phys. Lett. **89**, 223108 (2006); I. Levchenko, K. Ostrikov, M. Keidar, and S. Xu, J. Appl. Phys. **98**, 064304 (2005).
[45]S. Hofmann, C. Ducati, J. Robertson, and B. Kleinsorge, Appl. Phys. Lett. **83**, 135 (2003).
[46]X. Chen and S. Motojima, J. Mater. Sci. **34**, 5519 (1999).